PROCEEDINGS OF SCIENCE

ATLAS ITk Pixel Pre-production Planar Sensor Characterisation for the HL-LHC Upgrade

Yusong Tian,[a,*] **Giovanni Calderini,**[b] **Imogen Camp,**[a] **Thibaud Idriss Carcone,**[b] **Paul Mickael Chabrillat,**[b] **Artur Cordeiro Oudot Choi,**[b] **Francesco Crescioli,**[b] **Jörn Große-Knetter,**[a] **Šejla Hadžić,**[c] **Shunsuke Iizaka,**[d] **Christopher Krause,**[e] **Lingxin Meng,**[f] **Koji Nakamura,**[g] **Arnulf Quadt,**[a] **Stefano Terzo,**[h] **Ana Sofia Torrento Coello**[i] **and Hua Ye**[a]

[a] *II. Physikalisches Institut, Georg-August-Universität Göttingen, Friedrich-Hund-Platz 1, DE - 37077 Göttingen, Germany*

[b] *LPNHE, Sorbonne Université, Université Paris Cité, CNRS/IN2P3, 4 place Jussieu, FR - 75005 Paris, France*

[c] *Max-Planck-Institut für Physik (Werner-Heisenberg-Institut), Föhringer Ring 6, DE - 80805 München, Germany*

[d] *Division of Physics and Tomonaga Center for the History of the Universe, Faculty of Pure and Applied Sciences, University of Tsukuba, 1 Chome-1-1 Tennodai, Tsukuba, Japan*

[e] *Fakultät Physik, Technische Universität Dortmund, Otto-Hahn-Straße 4, DE - 44227 Dortmund, Germany*

[f] *Physics Department, Lancaster University, Bailrigg, Lancaster LA1 4YW, United Kingdom*

[g] *KEK, High Energy Accelerator Research Organization, 1-1 Oho, Tsukuba, Japan*

[h] *Institut de Física d'Altes Energies (IFAE), Barcelona Institute of Science and Technology, UAB Campus, Edifici CN, ES - 08193 Barcelona, Spain*

[i] *Detectors and Instrumentation Department, IJCLab – Laboratoire de Physique des 2 Infinis Irène Joliot-Curie, UMR 9012 – CNRS / Université Paris-Saclay / Université Paris Cité, 15 rue Georges Clémenceau, FR - 91405 Orsay, France*

E-mail: yusong.tian@uni-goettingen.de

*Speaker

PoS(Pixel2022)067

In the ATLAS detector upgrade for the High-Luminosity LHC (HL-LHC), the current Inner Detector will be replaced with an all-silicon Inner Tracker (ITk), to operate under higher occupancy (instantaneous luminosity 7.5×10^{34} $\mathrm{cm}^{-2}\mathrm{s}^{-1}$, which corresponds to about 200 inelastic pp collisions per bunch crossing) and radiation damage (particle fluence up to 2×10^{16} $\mathrm{n_{eq}/cm^2}$). The data taking is planned to start in 2029 and last for 10 years. The innermost part of the ITk will be equipped with pixel modules, consisting of pixel sensors and novel ASICs, implemented in 65 nm CMOS technology. The ITk project is currently in pre-production stage. To assure that specifications will be met during production, sensors and test structures from different vendors were sent to different sites for irradiation, hybridisation and follow-up testing. This paper presents the results of the characterisation of the pre-production planar sensor for ITk.

10th International Workshop on Semiconductor Pixel Detectors for Particles and Imaging (Pixel2022), 12-16 December 2022
Santa Fe, New Mexico, USA

1. Introduction

The Large Hadron Collider (LHC) at CERN will undergo an upgrade to High Luminosity LHC (HL-LHC) in the years 2025 to 2028, to continue and enable more experimental particle physics studies, and unveil principles of fundamental physics. The HL-LHC will reach an instantaneous luminosity of 7.5×10^{34} cm^{-2} s^{-1}, which corresponds to an average pile-up of about 200 inelastic pp collisions per bunch crossing (25 ns) [1]. To deal with the higher occupancy and harsher radiation environment of 2×10^{16} n_{eq}/cm^2 particle fluence, the ATLAS detector is also going to be upgraded. During the ATLAS detector upgrade, the Inner Detector will be replaced with an all-silicon **I**nner **T**rac**k**er (ITk). See Figure 1 for the layout of the ITk. The ITk consists of the pixel detector and the strip detector, with the pixel detector being the innermost part. It is more radiation-hard, has better granularity, and the acceptance of $|\eta|$ is increased from <2.5 to 4 [2, 3]. The planned data taking after the upgrade is from 2029 to 2039.

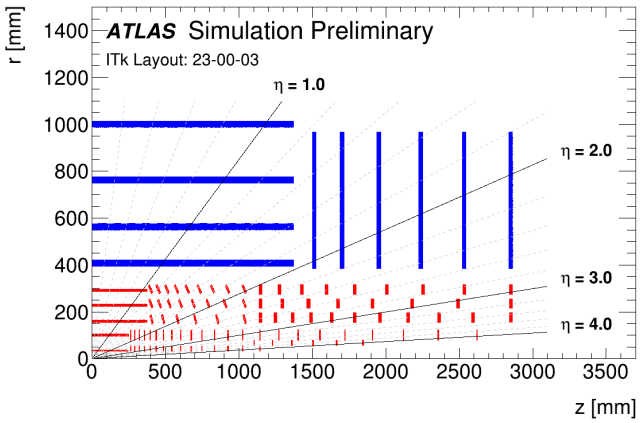

Figure 1: Layout of one quadrant of the ITk. The pixel detector is shown in red, it consists of 5 layers of flat barrels and inclined rings (which are referred to as L0 to L4) and 5.5 layers of end-cap rings (R0, R0.5 to R4) [4].

2. Planar Sensor of the ATLAS ITk Pixel Detector

2.1 The Sensors

The pixel detector contains hybrid modules made of sensor tiles bump-bonded with front-end read-out electronics (FE), and assembled to a flexible printed circuit board referred to as a "flex". Two types of modules will be used: quad modules and triplet modules. Quads consist of four FEs bump-bonded to a 4×4 cm^2 sensor tile, and triplets are made of three FEs, each bump-bonded to a 2×2 cm^2 sensor tile. Figure 2 shows the schematics of the cross section of a quad module.

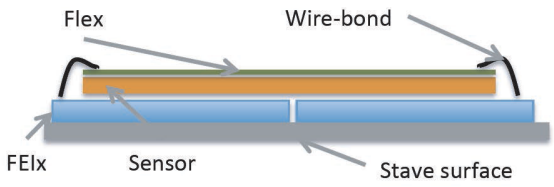

Figure 2: Schematics of a hybrid quad module [3]. The sensor is bump-bonded to 4 FEs and glued to a flex, and the flex is wire-bonded to the FEs.

Different technologies are used for the sensors: 3D and planar. 3D sensors have n^+-type and p-type columns in p-type substrate, planar sensors are n^+-in-p type (n^+-type implants in p-type substrate). They will be used in different parts of the detector: 3D sensors were chosen for the inner layer, because they are more radiation-hard, and require lower bias voltage (lower power dissipation); planar sensors will be used for the outer layers, with the second closest to the interaction point (L1) using thinner sensors (100 µm instead of 150 µm as for the other outer layers), because they have less material budget and lower power dissipation, however, the downsides are the risks and complications of processing such thin substrates and the consequently larger production cost. The pixel pitch of the central part (barrel) of the innermost layer (L0) is $25 \times 100\,\mu m^2$, as opposed to $50 \times 50\,\mu m^2$ for the rest. Table 1 summarises the active thickness, position, pixel pitch and overall sensor size of different types of sensors in the pixel detector, and the types of modules into which they are planned to be assembled.

	Active Thickness	Position	Pixel pitch	Sensor Size	Module Type
Planar	150 µm	L2-4, R2-4	$50 \times 50\,\mu m^2$	$4 \times 4\,cm^2$	Quads
	100 µm	L1, R1			
3D	150 µm	R0-0.5	$50 \times 50\,\mu m^2$	$2 \times 2\,cm^2$	Triplets
		L0	$25 \times 100\,\mu m^2$		

Table 1: Planned positions of planar and 3D sensors in the pixel detector, parameters of the sensor tiles, and the types of modules into which they will be assembled [3, 4].

Three vendors were selected via a market survey and a tender to produce planar sensors: HPK, Micron and FBK. On each wafer there are quad sensor tiles and various of test structures (TS). The active thicknesses and bias structures used by the vendors, as well as the numbers of quad sensor tiles per wafer are shown in Table 2.

Vendor	Active Thickness	Bias Structure	Sensor Tiles per Wafer
HPK	150 µm	Poly-Si	6
Micron	150, 100 µm	Punch-through	5
FBK	100 µm	None (temporary metal)	5

Table 2: Planar sensors with different active thicknesses and bias structures produced by different vendors, and the numbers of quad sensor tiles produced on each wafer. FBK sensors will have no permanent bias structure but temporary metal deposition, making it possible to take e.g. leakage current (IV) measurements. The temporary metal will be removed before further processing of the sensors like hybridisation.

It is planned to use the TS to monitor the quality during production. Figure 3 shows an example of a die with TS from HPK, and a quad sensor from Micron (150 µm). The sizes of the die and quad sensor tile in this picture are not adjusted to the actual proportion. For the rest of this paper, the word "sensor tile" will be used to refer to full-size pixel sensors that could be assembled into ITk modules, while "sensor" will be used in general to refer to both sensor tiles and TS.

2.2 Pre-production Quality Assurance

The ATLAS ITk pixel detector upgrade is currently in pre-production stage. In this stage, a small fraction of sensors are procured from the different vendors to make sure that they meet the

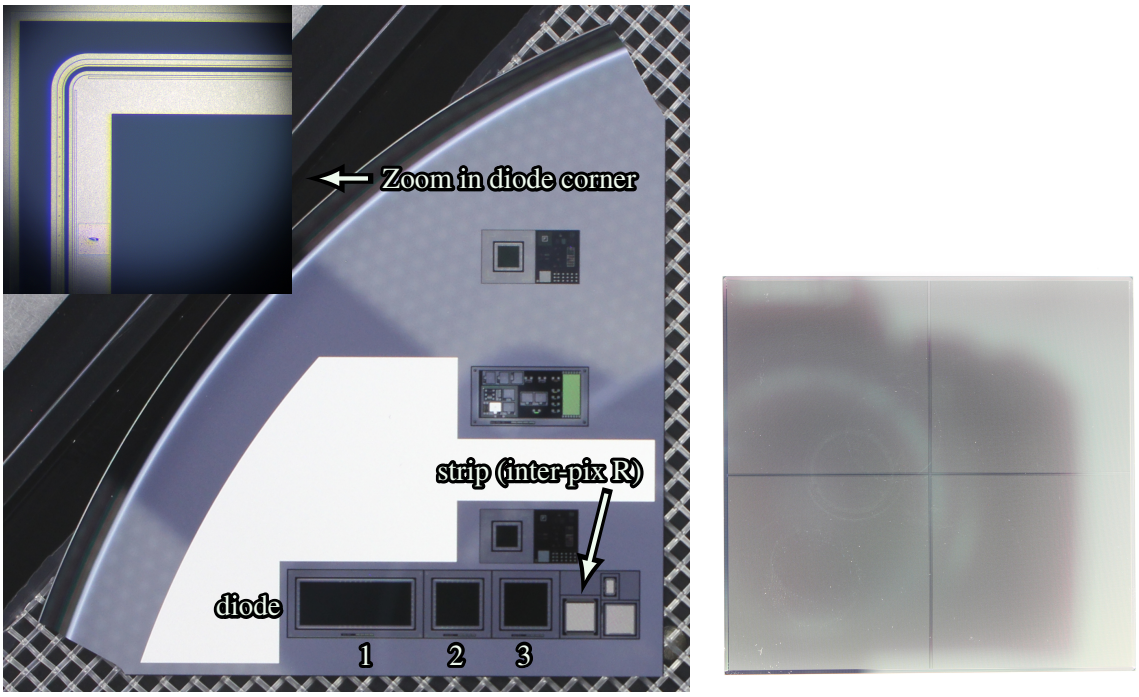

(a) HPK test structures

(b) Micron sensor tile

Figure 3: HPK TS with zoom-in photo of a diode, and a Micron sensor tile. The sizes between the TS die and the sensor tile is not to the actual proportion.

specifications for the final production. After the wafers are produced, the vendors would firstly do a quality control (QC): measure IV on all sensor tiles, and CV on part of sensor tiles/diodes. Some wafers are sent after dicing at the sensor or hybridisation vendors to different ITk testing sites for quality assurance (QA), and are accepted if both QC and QA meet the requirements. Some go through under-bump-metallisation, dicing, and bump-bonding at the hybridisation vendors. For QA, the characterisation of the sensors is done by these tests:

- Basic measurements performed on sensor tiles and diodes:
  - IV - leakage current as a function of reverse bias voltage
  - CV - bulk capacitance as a function of reverse bias voltage
  - It - leakage current stability
  - Visual inspection and metrology
- Additional measurements performed on dedicated test structures:
  - Inter-pixel resistance, inter-pixel capacitance
  - Charge collection efficiency
  - Other technological TS (e.g. poly-Si resistance)

Currently the QA is ongoing. Sensor tiles and diodes are used for IV, CV and It measurement, the strip TS are used for inter-pixel resistance. HPK and Micron sensors were tested both before and after irradiation, FBK testing and irradiation is in progress. The measurements reported in this paper are QA tests of the pre-production planar sensors, focusing on IV, CV, It and inter-pixel R.

Results for other optional tests will not be discussed in this paper. The specification for the relevant measurements is summarised in Table 3.

Leakage current	Un-irrad		<0.75 µA/cm^2 at V_{dep}+50 V
	Irrad	150 µm	<45 µA/cm^2 at 600 V
		100 µm	<35 µA/cm^2 at 400 V
Breakdown voltage	Un-irrad		>V_{dep}+70 V
	Irrad	150 µm	>600 V
		100 µm	>400 V
Depletion voltage	Un-irrad	150 µm	<100 V
		100 µm	<60 V
It fluctuation			<25 %
Inter-pixel R		Poly-Si bias rail	>2 MΩ
		Other permanent bias structures	>20 MΩ

Table 3: The specification. Leakage current (also in It) should be tested at 20±1 °C before irradiation, and after irradiation at -25±1 °C after annealing at room T for 10 days. The relative humidity should be <50 %. The irradiated requirements are for sensors irradiated with 5×10^{15} n_{eq}/cm^2, limits for 2×10^{15} n_{eq}/cm^2 are omitted.

2.3 Testing Setup

The testing was done at multiple sites including IJCLab, KEK, MPP, TU Dortmund, University of Göttingen, and Lancaster University. The testing setup used at Göttingen is presented here as an example. Various voltage sources and meters were used for different measurements, as shown in Table 4. Keithley6487 was used for CV measurements because Keithley2410 source meters were found to be incompatible with the CV setup. The sensors were put in a probe station for probing, and the temperature of the chuck in the probe station was controlled by a chiller, to reach the required temperature 20±1 °C for leakage current measurements on un-irradiated sensors, and -25±1 °C on irradiated ones. The environmental monitoring is done by a PT1000 temperature sensor connected to the chuck via kapton tape, an NTC temperature sensor and a HIH4000 relative humidity sensor placed close to the chuck. Figure 4 shows photos of the probe station and the chiller.

Tests	Voltage Source	I or C Meter
IV, It	Keithley2410	Keithley2410 or 6487
Inter-pixel R	Keithley2410	Keithley6487
CV	Keithley6487	HM8118 LCR bridge

Table 4: Voltage sources and meters.

3. Results

3.1 Leakage Current vs Bias Voltage (IV)

The IV measurement gives information on the breakdown status and the level of leakage current. The breakdown voltage V_{bd} is defined as the voltage at which the leakage current I increases by

(a) Probe station: Süss PA300 **(b)** Chiller and controller: Huber Unistat 380

Figure 4: The probe station and the chiller. The probe station has inlets for connection to dry air for humidity control, and vacuum for fixing the sensor on the chuck. It also provides shielding from the ambient light. The temperature of the chuck is controlled by the chiller.

>20% in 5 V, excluding 0 to 5 V.
30 un-irradiated HPK diodes were tested in pre-production QA and 29 showed no breakdown, see Figure 5 for IV curves of nine diodes on wafer 5. These IV curves are from three TS dies, on each die there are one larger diode of size 5×10 mm^2 (labelled D1), and two small diodes of size 5×5 mm^2 (D2 and D3). Due to the size difference, D1s have almost double the leakage current of D2 and D3s. The leakage current level at V_{dep}+50 V (which is about 120 V) are all well within the limit set in the specification, which amounts to 375 nA for D1s, and 188 nA for D2 and D3s. The scale of these limits is too large to be shown in the figure. Sensor tiles from HPK and Micron were also tested to ensure that the measurements made by the vendor can be reproduced. Testing results showed good agreement.

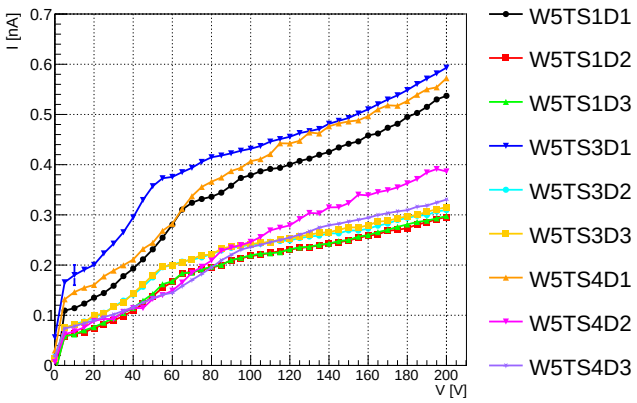

Figure 5: IV of nine un-irradiated HPK diodes from wafer 5. Diodes on three TS dies were tested, on each die there are three diodes, the diodes labelled D1 are of size 5×10 mm^2, D2 and D3 are of size 5×5 mm^2.

Seven sensor tiles irradiated at fluence around 5×10^{15} n_{eq}/cm^2 were tested (Figure 6), The seven sensor tiles tested are all within specification, as indicated by the dashed red lines. The default size

of quad sensor tiles (41.1 mm × 39.5 mm) was used in the calculation of the I limit.

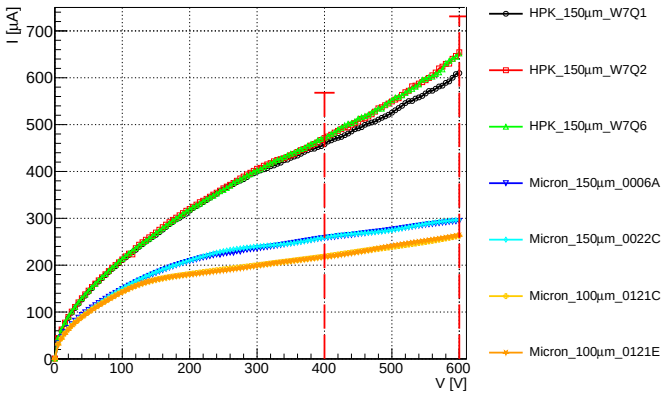

Figure 6: IV curves of irradiated sensor tiles. All the measurements are within specification, as indicated by the dashed red lines: the limit on I is at 400 V for 100 µm sensors and at 600 V for 150 µm sensors, the short horizontal lines on the top of the dashed lines indicate the I limit calculated using the default size of quad sensor tiles.

3.2 Capacitance vs Bias Voltage (CV)

The capacitance of sensors affects the noise at the preamplifier on the FE, and the full depletion voltage V_{dep} can be obtained from plotting $\frac{1}{C^2}$ against the reverse bias voltage and fitting two straight lines to the ramp and the plateau, the voltage that corresponds to the intersection point is V_{dep}.
Figure 7 shows the result of HPK diodes on dies from two different wafers, tested by two different testing sites. The capacitance decreases fast at low bias voltage, D1s have about double the capacitance of D2 and D3s due to the difference in size. There is a slight shift between the results for the same-sized diodes on dies from different wafers tested by different testing sites, which can be explained by differences between wafers and the testing setups. There are two kinks in the $\frac{1}{C^2}$ plot possibly due to edge effects: there are extra p^+-doped rings outside the active area of the diodes, which causes further lateral depletion. Thus the first intersection point with lower V reflects better the V_{dep} needed to deplete the sensors across the whole thickness. The CV curves for Micron sensor tiles are shown in Figure 8, sensor tiles on wafer 0016 were tested without dicing. There is no edge effect observed on the sensor tiles, possibly due to their larger area compared to diodes, which makes the edge effect negligible.
The V_{dep} obtained from HPK diodes is 55 to 62 ± 5 V, the uncertainty is estimated by varying the data points that are included in the fit. V_{dep} for Micron sensors is 64 to 67 V for 150 µm and 43 to 45 V for 100 µm sensors. The results all meet specification, as indicated by the dashed red lines.

3.3 Leakage Current Stability (It)

It curves were taken by measuring the leakage current every 10 minutes for 48 hours, skipping the first 10 min. The diodes were biased at V_{dep} + 50 V, which is the operating voltage. This is to test if the leakage current is stable during operation. The fluctuation is defined as $\frac{\text{max}-\text{min}}{\text{average}}$ and is required

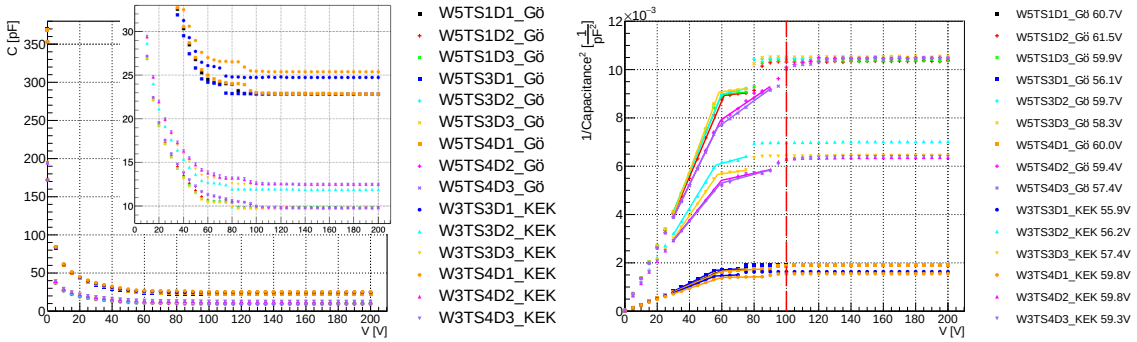

(a) **(b)**

Figure 7: CV and $\frac{1}{C^2}$ of HPK diodes. The overlayed figure in (a) is a zoom-in of the lower C region. Diodes named D1 are larger (5×10 mm^2) than D2 and D3 (both 5×5 mm^2). The results are from two different testing sites: Göttingen and KEK, each site tested dies from a different wafer. The full-depletion voltages V_{dep} written in the legend are the voltages correspond to the first intersection point (with lower V) of the fitted lines. The dashed red line indicates the limit on V_{dep} required by the specification.

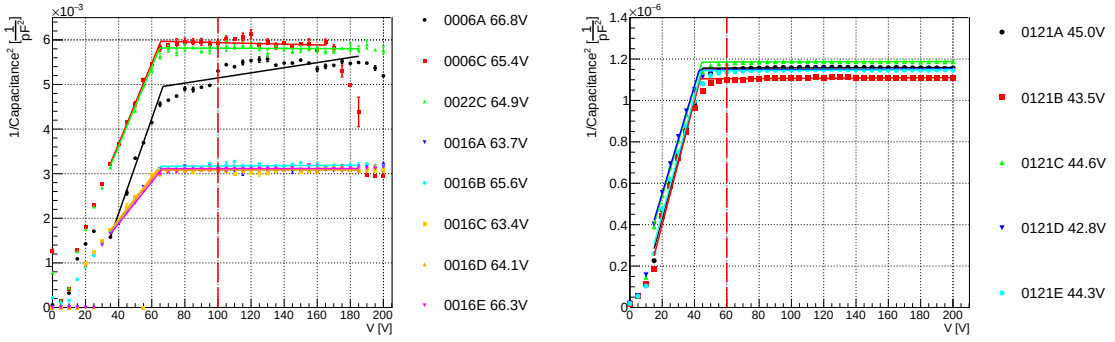

(a) Micron 150 µm **(b)** Micron 100 µm

Figure 8: CV of Micron sensors with two active thicknesses. The V_{dep} obtained from each CV curve is written in the legend, and the required limit is indicated by the dashed red lines.

to be within 25 %. Figure 9 shows the result for HPK un-irradiated diodes, all measurements showed fluctuation within the limit.

However, un-irradiated Micron sensor tiles showed unstable behaviour, as shown in Figure 10a. The 100 µm sensor tile named 0121D was tested at two different bias voltages (90 V and 70 V) at 20 °C chiller T. When biased at 90 V, the It curve shows fast increase then decrease, while a shorter measurement at 70 V showed only increase and no obvious decrease. The fluctuations for both curves are higher than the required limit. The result of 150 µm only decreases and is also over the limit (figure omitted for simplicity).

This effect is gone after irradiation, as shown in figure 10b on measurements done on two sensor tiles irradiated with 5×10^{15} n_{eq}/cm^2 fluence and a diode irradiated with 2×10^{15} n_{eq}/cm^2. The fluctuations are small despite the measurement of 0006A having suffered from fluctuating chiller T, and having biased the diode 0121TSB3 at a very high voltage (400 V). It is suspected that the

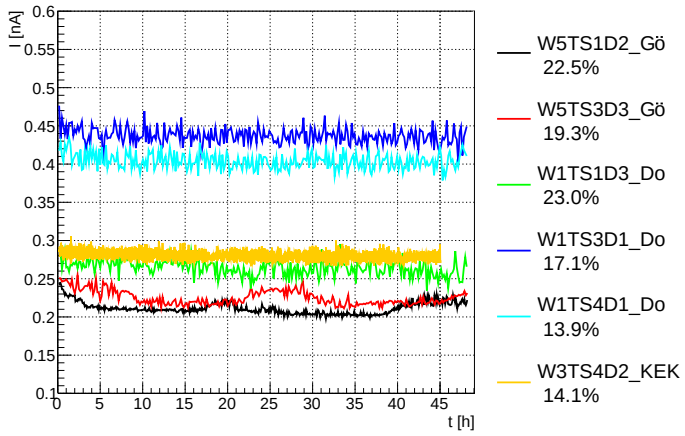

Figure 9: HPK It curves. The current is not corrected for temperature fluctuation. The curve for W5TS1D2 and W5TS3D3 shows periodic fluctuation, which is likely from environmental influence like ambient light. The fluctuations of all the curves are written in the legend and are within limit.

change of leakage current in un-irradiated sensor tiles is due to a surface effect.

The vendor suggested baking the sensors (125 °C for 16 hours, and flush the sensor for 2 to 3 h with dry N_2 if the sensor has been staying in an environment with relative humidity >50 % before baking) to eliminate this effect. This suggestion is consistent with the practice in the strip detector community (150 °C for 15 hours with no special environment). Follow up testing will be done to investigate this.

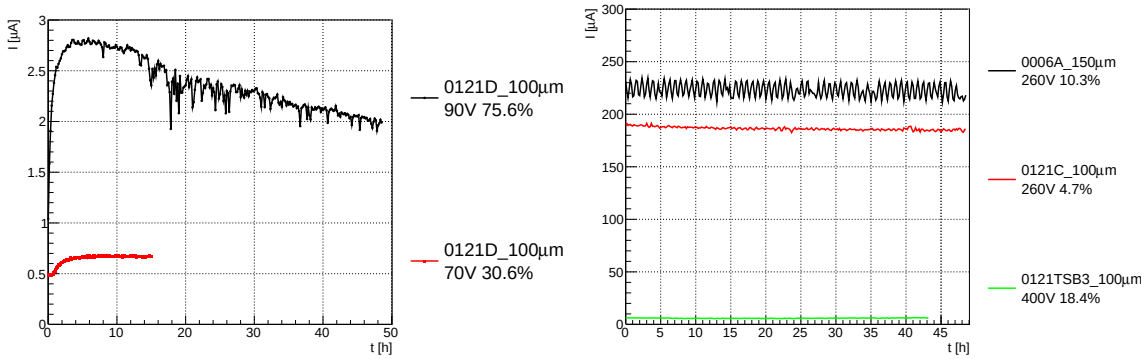

(a) Micron 100 µm un-irrad sensor tile It

(b) Micron 150 µm and 100 µm irrad It

Figure 10: It curves for un-irradiated and irradiated Micron sensors. For un-irradiated 100 µm sensor tile 0121D (figure a), I increases fast and then decreases steadily w.r.t. time when biased at 90 V. A shorter curve was obtained at 70 V, in this case I still increases but no obvious decrease is observed. The fluctuation, as written in the legend, is out of specification in both cases. Two sensor tiles irradiated with 5×10^{15} n_{eq}/cm^2 fluence (0006A and 0121C) and one diode irradiated with 2×10^{15} n_{eq}/cm^2 (0121TSB3) were tested after irradiation (figure b), and the problem with un-irradiated sensor tile is no longer visible. The wavy fluctuation in 0006A is due to temperature fluctuation of the chiller.

3.4 Inter-Pixel Resistance

Inter-pixel resistance was measured to test the inter-pixel isolation. The measurements were done on the HPK strip TS, a photo and the wafer map is shown in Figure 11a. The TS consists of pixels connected together, forming strips. There are 40 connected pixels per strip, and 40 strips in total on one TS. For HPK strip TS, there are pads at both ends of each strip for probing.
The measurements were done by placing two probe needles on the neighbouring strips and applying voltage. Probing the pads on the same or different ends of two strips made no visible difference.
The current vs voltage was measured in a small voltage range around 0 V. When applying voltage across the two strips, the 40 pixels are connected in parallel. Since 20 of the pixels are connected by poly-Si bias rail which results in much smaller resistance, the current from the other pixels are considered negligible. This means R can be obtained by dividing the measured current by 20 and plotting it against the voltage. After fitting a straight line to the linear part, Ohm's law gives that R is inverse the slope. The results show that R~5 MΩ (Figure 11b), which meets the requirement. The TS were not biased in these measurements, giving a more conservative measurement of R [5]. The measurement of Micron strip TS is ongoing.

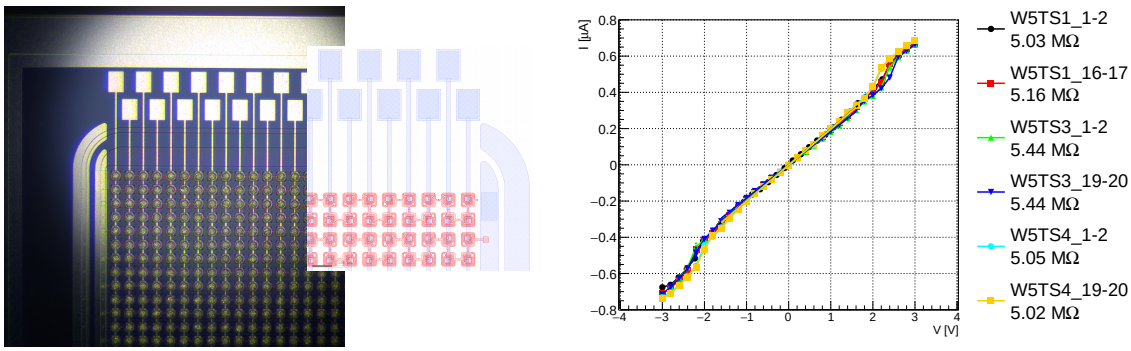

(a) HPK strip TS photo and layout

(b) Inter-pixel R, tested on HPK strip TS

Figure 11: HPK strip test structure and testing results. Detail of the poly-Si bias rail is shown in red on the TS layout, half of the pixels on the neighbouring strips are connected by them. Two pairs of strips on each of the three TS on wafer 5 were tested, the indices of the strips are indicated in the legend, e.g. 1-2 being the first two strips next to the edge of the TS. Result shows that R~5 MΩ independent of the location of the strip.

4. Conclusions & Outlook

The sensor pre-production for the ATLAS ITk pixel detector upgrade for the HL-LHC is ongoing, several QA testing sites tested sensor tiles and test structures before and after irradiation. For planar sensors, results for the electrical tests meet the requirements in the specification or are consistent with vendor QC measurements, except for the unstable leakage current problem found in the un-irradiated sensor tile It of one vendor. Follow-up testing is ongoing. The sensors from the other vendors recently passed the production readiness review and will move into production. The ITk sites are going to continue with the testing to get more statistics on It, and test inter-pixel C and FBK sensors.

References

[1] G. Apollinari et al., *High-Luminosity Large Hadron Collider (HL-LHC): Technical Design Report V. 0.1*, CERN Yellow Reports: Monographs, CERN, Geneva (2017), 10.23731/CYRM-2017-004.

[2] ATLAS collaboration, *The ATLAS Experiment at the CERN Large Hadron Collider*, *JINST* **3** (2008) S08003.

[3] ATLAS collaboration, *Technical Design Report for the ATLAS Inner Tracker Pixel Detector*, CERN-LHCC-2017-021, ATLAS-TDR-030, https://cds.cern.ch/record/2285585, CERN, Geneva (2017).

[4] ATLAS collaboration, *Expected tracking and related performance with the updated ATLAS Inner Tracker layout at the High-Luminosity LHC*, ATL-PHYS-PUB-2021-024, http://cds.cern.ch/record/2776651, CERN, Geneva (2021).

[5] M.S. Alam et al., *The ATLAS Silicon Pixel Sensors*, 16, https://cds.cern.ch/record/683924, CERN, Geneva (2001).

Acknowledgments

Part of this work was supported by the Federal Ministry of Education and Research (BMBF), FIS under contract number 05H21MGCA9.